We are IntechOpen, the world's leading publisher of Open Access books
Built by scientists, for scientists

4,800
Open access books available

122,000
International authors and editors

135M
Downloads

Our authors are among the

154
Countries delivered to

TOP 1%
most cited scientists

12.2%
Contributors from top 500 universities

CLARIVATE ANALYTICS
BOOK CITATION INDEX
INDEXED

WEB OF SCIENCE™

Selection of our books indexed in the Book Citation Index in Web of Science™ Core Collection (BKCI)

Interested in publishing with us?
Contact book.department@intechopen.com

Numbers displayed above are based on latest data collected.
For more information visit www.intechopen.com

3

Use of Proper Closure Equations in Finite Volume Discretization Schemes

A. Ashrafizadeh, M. Rezvani and B. Alinia
K. N. Toosi University of Technology
Iran

1. Introduction

Finite Volume Method (FVM) is a popular field discretization approach for the numerical simulation of physical processes described by conservation laws. This article presents some advances in finite volume discretization of heat and fluid flow problems.

In the case of thermo-fluid problems, decision regarding the choice of unknown variables needs to be taken at the continuous level of formulation. A popular choice, among many available options, is the pressure-based primitive variable formulation (Acharya, 2007), in which the flow continuity equation is considered as a constraint on fluid pressure. Pressure-based finite volume methods, in turn, can be categorized based on the computational grid arrangement used for the discretization of solution domain. In a staggered grid arrangement, velocity components and other unknown scalars are defined at different nodal points (Patankar, 1980). On the contrary, all unknown variables are defined at the same nodal locations in a co-located grid arrangement. The discussion of finite volume discretization schemes in this article is limited to pressure-based formulations on co-located grids.

At the continuous level of formulation in a finite volume method, an intensive variable φ is constrained by an integral balance equation for a control volume CV bounded by the control surface CS as follows:

$$\frac{\partial}{\partial t}\iiint_{CV}\rho\varphi dV+\oiint_{CS}\vec{J}_{\varphi}\bullet\vec{n}dA=\iiint_{CV}\dot{S}_{\varphi}dV \tag{1}$$

In Eq. (1) $\vec{J}_{\varphi}$ represents the flux of φ across the control surface, $\dot{S}_{\varphi}$ stands for the rate of generation of φ within the control volume and $\vec{n}$ is the outward unit normal vector to the control surface. In most of the engineering problems of interest, there are two mechanisms for the transport of φ, i.e. advection and diffusion, and the flux function is mathematically described as follows:

$$\vec{J}_{\varphi}\equiv\left(\rho\vec{V}\right)\varphi-\left(\Gamma_{\varphi}\right)\vec{\nabla}\varphi \tag{2}$$

In Eq. (2) $\rho\vec{V}$ is the advective mass flux and Γ_{φ} is the diffusion coefficient associated with variable φ. By properly defining φ, $\vec{J}_{\varphi}$ and $\dot{S}_{\varphi}$, Eq. (1) can be used as a generic equation to

mathematically describe the transport of mass, momentum and energy in fluid flow problems (Patankar, 1980).

A typical two dimensional discrete domain covered by contiguous control volumes (cells) is shown in Fig. 1. Each cell represents a nodal point and is bounded by a number of panels which comprise the control surface. Typically, each panel includes one integration point. There isn't any limitation on the shape and the number of panels of a cell. Here we use a background finite element mesh to define the control volumes. Figure 1 shows structured and unstructured two-dimensional grids in an element-based finite volume method (EBFVM) context (Ashrafizadeh et al., 2011).

The objective of any finite volume discretization scheme is to use the CV balance equations, similar to Eq. (1), to obtain a set of algebraic equations which constrains the unknown nodal values throughout the domain. This objective is achieved by carrying out the discretization in two stages.

At the first stage of discretization, here called level-1 approximation, Eq. (1) is converted to a semi-discrete form comprising of both nodal and integration point variables. Level-1 approximate form of Eq. (1) for an internal finite volume in Fig. 1 can be written as follows:

$$\frac{\Delta(\rho\varphi)_{np}}{\Delta t}\delta V + \sum_{ip=1}^{N_{ip}} (\rho\varphi\vec{V} \bullet \vec{n}dA)_{ip} = \sum_{ip=1}^{N_{ip}} (\Gamma_{\varphi}\frac{\partial\varphi}{\partial n}A)_{ip} + \dot{S}\varphi\delta V \tag{3}$$

In Eq. (3), subscripts np and ip stand for nodal and integration point variables respectively. Closure equations are now needed to relate ip variables to np variables.

At the second stage of discretization, here called level-2 approximation, Eq. (3) is converted to a fully-discrete form, i.e. an algebraic equation which constrains the variable φ at nodal point P. The computational molecule obtained at this stage of discretization is written in the following convenient form:

$$a_P\varphi_P = \sum_{nb=1}^{N_{nb}} a_{nb}\varphi_{nb} + S_P^{\varphi} \tag{4}$$

Here, subscript nb stands for the neighbor nodes and superscript N_{nb} refers to the number of influential neighbor nodes. Influence coefficients a_P and a_{nb} and the source term S contain terms and parameters which model all physical effects relevant to the value of φ at the nodal point P.

If Eq. (1) is a nonlinear equation, linearization also becomes necessary and should be carried out during the discretization. In principle, the equation can be linearized before or after each of the approximation levels and this might affect the properties of the final discrete model.

In most engineering problems, including heat and fluid flow ones, a coupled set of nonlinear partial differential equations needs to be discretized and solved. In such cases, the inter-equation couplings should also be numerically modeled. Two-dimensional, incompressible Navier-Stokes equations, for example, can be written in a form similar to Eq. (1) in which φ is equal to 1 in the mass balance equation, u in the x-momentum balance equation, v in the y-momentum balance equation and e (specific energy) in the energy

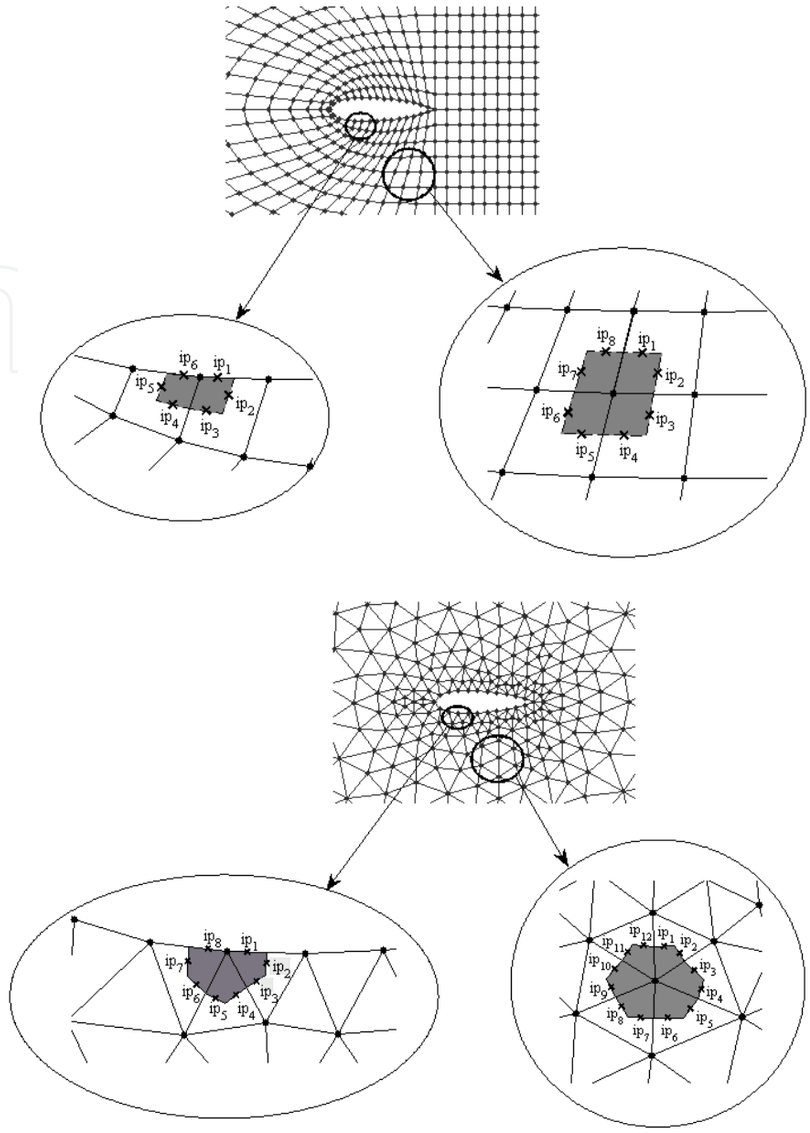

Fig. 1. Structured and unstructured element-based finite volume grids.

balance equation. In general, the computational molecule associated with each equation of a coupled set includes more than one variable to reflect the fact that the equations and the variables are inter-related. Therefore, in the case of a set of equations with two coupled variables φ and ψ, the following modified form of Eq. (4) is used to constrain φ at the nodal point P:

$$a_P^{\varphi}\varphi_P = \sum_{nb=1}^{N_{nb}} a_{nb}^{\varphi}\varphi_{nb} + a_P^{\psi}\psi_P + \sum_{nb=1}^{N_{nb}} a_{nb}^{\psi}\psi_{nb} + S_P^{\varphi} \tag{5}$$

In this article, we focus on level-2 approximation of Navier-Stokes equations in the context of co-located, pressure-based finite volume method. This level of approximation is particularly important because it deals with the modeling of physical influences such as upwind and

downwind effects and the couplings between variables. A number of famous level-2 approximations are reviewed and the method of proper closure equations (MPCE), proposed by the first author, is introduced. To avoid the complexities associated with multi-dimensional problems and to focus on the nature of the approximations in a simple setting, one dimensional equations and test cases are discussed in details. Two-dimensional results are only briefly presented to show the applicability of the MPCE in multi-dimensional problems.

2. The semi-discrete form of equations in a 1D context

A one-dimensional variable-area duct is shown in Fig. 2. The complete set of governing equations for unsteady 1D-inviscid compressible flow in this duct, using the momentum variable formulation, is as follows (Chterental, 1999):

$$\frac{\partial}{\partial \tau}\begin{bmatrix}\rho\\ f\\ \rho e\end{bmatrix}+\frac{\partial}{\partial x}\begin{bmatrix}f\\ fu+p\\ fe+pu\end{bmatrix}=\begin{bmatrix}-f\dfrac{1}{a}\dfrac{da}{dx}+S^m\\ -fu\dfrac{1}{a}\dfrac{da}{dx}+S^u\\ -pu\dfrac{1}{a}\dfrac{da}{dx}\end{bmatrix} \tag{6}$$

Where τ is time, $f=\rho u$ is the momentum variable, u is velocity, p is pressure and a is the cross sectional area. Note that no artificial energy source term is used in the energy equation.

In order to close the above set of equations, an auxiliary equation is needed. Here, the ideal gas equation of state is used:

$$p=\rho R t \tag{7}$$

Where t is temperature and R is the gas constant. Neglecting the potential energy term, the total energy per unit mass (e) of an ideal gas can be written as follows:

$$e=c_v t+\frac{1}{2}u^2 \tag{8}$$

Where c_v is the specific heat at constant volume.

By integrating Eq. (6) over the P control volume in Fig. 2 and after using divergence theorem, the semi-discrete forms of the governing equations are obtained as follows:

$$\begin{bmatrix}\dfrac{V_P}{\Delta\tau}\left(\rho-\rho^{\circ}\right)_P+f_e a_e-f_w a_w\\ \dfrac{V_P}{\Delta\tau}\left(F_P-F_P^{\circ}\right)+\left[fu+p\right]_e a_e-\left[fu+p\right]_w a_w+P_P(a_w-a_a)\\ \dfrac{V_P}{\Delta\tau}\left((\rho E)-(\rho E)^{\circ}\right)_P+\left[fe+pu\right]_e a_e-\left[fe+Pu\right]_w a_w\end{bmatrix}=\begin{bmatrix}S_P^m V_P\\ S_P^p V_P\\ 0\end{bmatrix} \tag{9}$$

Note that capital letters (like F and P) are used for the nodal values and small letters (like f and p) are used for integration point variables. Here, V_P stands for the volume of cell P. Closure equations for the integration point variables are discussed next.

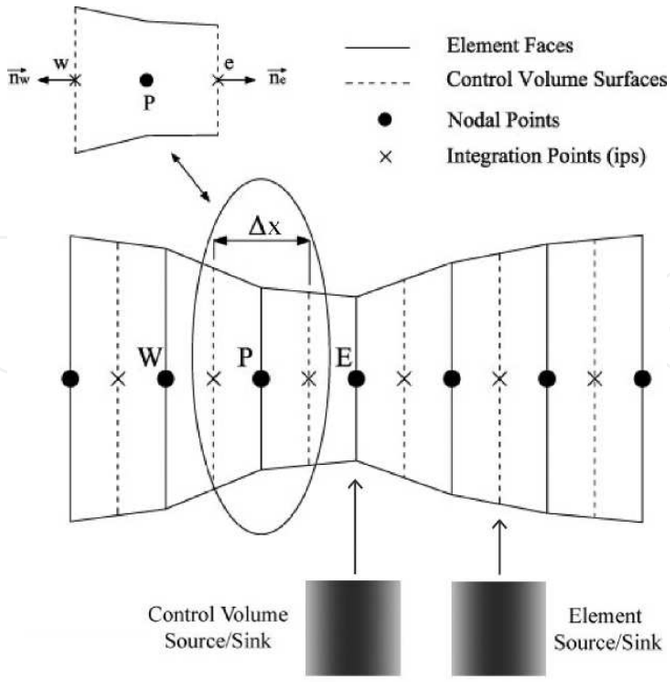

Fig. 2. Grid arrangement in a one-dimensional variable area duct.

3. Closure equations for integration point variables

After obtaining the semi-discrete form of governing equations and linearizing them, closure equations are needed to approximate integration point (ip) quantities in terms of the nodal values. By employing these closure equations, the semi-discrete equations are converted to fully-discrete equations. These ip-equations play a critical role in the robustness and accuracy of a collocated scheme. Therefore, different solution strategies for defining ip-equation are briefly described in this section. Here, we only discuss the closure equations for "east" integration point of a typical cell around node P. The closure equations at the "west" ip are obtained similarly.

3.1 Methods based on geometrical interpolation

Simple symmetric interpolation is the most trivial choice for an ip-value in a uniform grid:

$$\varphi_e = \frac{\phi_P + \phi_E}{2} \tag{10}$$

On non-uniform grids, weighted interpolation is used as follows:

$$\varphi_e = \lambda_e \phi_E + (1 - \lambda_e)\phi_P \tag{11}$$

Where λ_e is the weight factor for "east" ip, calculated by the following formula:

$$\lambda_e = \frac{x_e - X_P}{X_E - X_P} \tag{12}$$

This scheme is 2nd-order accurate, but is unbounded so that non-physical oscillations may appear in regions with high gradients. To show the problem associated with this scheme, consider the 1-D inviscid incompressible flow in a constant area duct shown in Fig. 3. The semi-discrete form of continuity and momentum equations in this case are as follows:

$$\rho A\left(u_e - u_w\right) = 0 \tag{13}$$

$$\bar{\dot{m}}\left(u_e - u_w\right) - A\left(p_e - p_w\right) = 0 \tag{14}$$

Where A is the cross sectional area of the duct and $\bar{\dot{m}}$ is the mass flow rate based on the most recent available value of velocity.

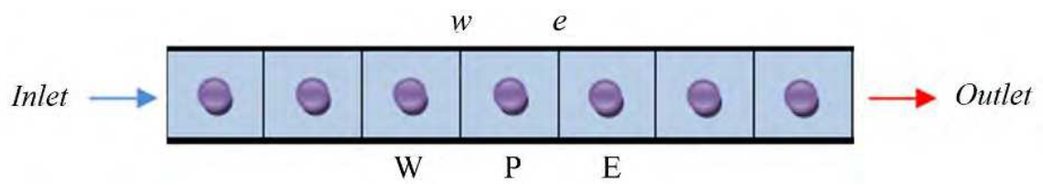

Fig. 3. A 1-D Co-located grid in a constant cross sectional area duct.

Using simple symmetric interpolation, Eqs. (13) and (14) are converted to the following fully-discrete forms:

$$\frac{\rho A}{2}\left(U_E - U_W\right) = 0 \tag{15}$$

$$\frac{\bar{\dot{m}}}{2}\left(U_E - U_W\right) - \frac{A}{2}\left(P_E - P_W\right) = 0 \tag{16}$$

Combining the above equations, one obtains the following constraint on the pressure at nodal point P:

$$P_E = P_W \tag{17}$$

Note that pressure at node P is absent in this equation and this constraint cannot distinguish between a uniform pressure field and the wiggly pressure field shown in Fig. 4.

3.2 Methods based on taylor-series expansion

It is logical to assume that convected quantities in a thermo-fluid problem are influenced by the upstream condition. Therefore, assuming the flow direction from P to E, the following truncated Taylor series expansions are both valid approximations for φ_e :

$$\varphi_e \approx \phi_P \tag{18}$$

$$\varphi_e \approx \phi_P + \left.\frac{\partial \varphi}{\partial x}\right|_P \left(x_e - X_P\right) \tag{19}$$

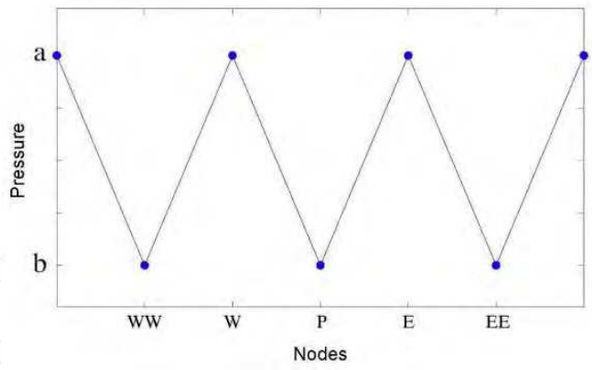

Fig. 4. A typical wiggly pressure filed.

Equation (18) is called the simple or Fist Order Upwinding (FOU) and provides highly stable and unconditionally bounded numerical schemes. However, it is only first order accurate. Equation (19) provides a Second Order Upwinding (SOU) strategy. One can show that a numerical scheme which employs Eq. (10) for integration point pressures and Eqs. (18) or (19) for integration point velocities in Eqs. (13) and (14), would not be able to detect the checkerboard pressure fields. Such numerical schemes are prone to unphysical pressure-velocity decoupling symptom.

3.3 Methods based on momentum interpolation

Rhie and Chow (Rhie, 1983) employed a co-located grid to solve the flow field around an airfoil. To avoid nonphysical, wiggly numerical solutions, they came to the conclusion that different closure equations had to be used for the convecting or mass-carrying ($\hat{u}$) and convected or transported (u) velocity components at the integration points. The convecting velocity, used in the semi-discrete continuity equation, is linked to the pressure through a momentum interpolation procedure. Hence, this discretization scheme is called the Momentum Interpolation Method (MIM). As compared to the classical schemes on staggered grids, one may assume that nodal momentum balances are conceptually staggered to obtain closure equations for convecting velocity at integration points. The discrete momentum balance for node P can be written as follows:

$$a_P U_P - \sum a_{nb} U_{nb} + V_P \left.\frac{\partial P}{\partial x}\right|_P = 0 \qquad \Rightarrow \qquad U_P = \frac{\sum b_{nb} U_{nb}}{a_P} - \frac{V_P}{a_P}\left.\frac{\partial P}{\partial x}\right|_P \tag{20}$$

The convecting velocity at "e" is obtained by staggering the stencil of the "P" computational molecule to the "e" integration point:

$$\hat{u}_e = \left.\frac{\sum a_{nb} U_{nb}}{a}\right|_e - \frac{V_e}{a_e}\left.\frac{\overline{\partial P}}{\partial x}\right|_e \tag{21}$$

Which results in:

$$\hat{u}_e = \frac{U_P + U_E}{2} + \frac{\overline{d}_e}{2}\left(\left.\frac{\overline{\partial P}}{\partial x}\right|_P + \left.\frac{\overline{\partial P}}{\partial x}\right|_E - 2\left.\frac{\partial P}{\partial x}\right|_e\right) \tag{22}$$

Where

$$\bar{d}_e \equiv \frac{1}{2}\left(\frac{V_P}{a_P} + \frac{V_E}{a_E}\right) \tag{23}$$

The closure for the convected velocity, and any other transported variable, comes from an upwind scheme. The simplest option at the integration point e would be the FOU:

$$u_e = U_P \quad \text{if} \quad \vec{m}_e > 0 \tag{24}$$

The interpolation formula, Eq. (22), is not unique as explained in (Acharya, 2007) and one might successfully implement the idea using modified forms of this approach. The key point, however, is to use different closure equations for the convected and convecting velocity components. The convecting velocity should be properly related to the pressure field.

The closure equation for p_e has not been a matter of concern, at least for incompressible flows. Taking into account the elliptic behavior of the pressure, the following closure equation is used in the MIM:

$$P_e = \frac{P_E + P_P}{2} \tag{25}$$

This technique guarantees the required physical pressure-velocity coupling in the numerical model and prevents any wiggly solutions (Ashrafizadeh et al., 2009).

3.4 Methods based on physical influences

The pleasure of working with all variables on a single nodal position, as opposed to the pain of working with staggered grids limited to simple geometries, has made the MIM very popular. Therefore, attempts have been made to employ and improve the MIM for the solution of flows at all speeds. Schneider and Raw (Schneider & Raw, 1987a, 1987b) proposed the physical influence scheme to unify the integration point velocity interpolation formulas in co-located grids. They retained a unified definition for the integration-point velocity components, but argued that the closure for u_e should not be obtained solely by purely mathematical upwind schemes. They suggested the non-conservative form of the momentum equation to provide a closure for u_e :

$$\left[u\frac{\partial(\rho u)}{\partial x} + \rho u\frac{\partial u}{\partial x} + \frac{\partial P}{\partial x}\right] = 0 \tag{26}$$

The method, called the physical influence scheme, provides the following closure equation in the context of the 1-D test case:

$$u_e = \hat{u}_e = U_p + \frac{\Delta x}{2\rho\bar{u}_e}\frac{P_P - P_E}{\Delta x} \tag{27}$$

Where the over bar refers to the most recent available value in the nonlinear iterations. Equation (25) is used as the closure for p_e in this scheme.

While successfully implemented in a number of multidimensional viscous problems, the physical influence scheme fails to prevent pressure checkerboard problem in inviscid incompressible flows (Bakhtiari, 2008). This failure reinforces the belief that two definitions for convected and convecting velocities at integration points are necessary when the calculations are carried out on a co-located grid.

3.5 Methods based on modified physical influences

To fix the problem associated with the physical influence scheme, Karimian and Schneider (Karimian, 1994a) accept the notion of dual velocities at the integration points and employ a combination of momentum and continuity equations to provide a closure for the convecting velocity ($\hat{u}$):

$$\hat{u}_e = \frac{U_P + U_E}{2} - \frac{\Delta x}{2\rho \bar{u}_e}\left[\left(Momentum\ Error\right) - \bar{u}_e\left(Continuity\ Error\right)\right]_e \tag{28}$$

Which results in:

$$\hat{u}_e = \frac{U_P + U_E}{2} - \frac{P_P - P_E}{2\rho \bar{u}_e} \tag{29}$$

They also use Eq. (27) for convected velocity (u_e) and Eq. (25) as the closure for p_e . Numerical experiments with the 1-D test case show that this method works well and successfully suppresses any oscillatory numerical solution even in time-depended all speed flows (Karimian, 1994b). This method has also been extended to 2D flows on structured (Alisadeghi et al., 2011a) and unstructured (Alisadeghi et al., 2011b) grids.

Darbandi (Darbandi et al., 1997) proposed a pressure-based all speed method similar to the Karimian's method, in which the momentum components ($f = \rho u$) are used as the flow dependent variables instead of the velocity components (u). They used the following form of the momentum equation as the physical constraint on the integration point convected velocity:

$$\left[\frac{\partial f}{\partial \tau} + \bar{u}\frac{\partial f}{\partial x} + \bar{f}\frac{\partial u}{\partial x} + \frac{\partial P}{\partial x}\right]_e = 0 \tag{30}$$

Where $f = \rho u$ is the momentum variable. Appropriate discretization of Eq.(30) leads to:

$$f_e = F_P + \frac{1}{4\bar{u}_e}\left(P_P - P_E\right) \tag{31}$$

In this method, a combination of momentum and continuity equations is used to constrain the integration point convecting velocity:

$$\left[\frac{\partial f}{\partial \tau} + \bar{u}\frac{\partial f}{\partial x} + \bar{f}\frac{\partial u}{\partial x} + \frac{\partial P}{\partial x}\right]_e - \alpha \bar{u}_e\left[\frac{\partial \bar{\rho}}{\partial \tau} + \frac{\partial f}{\partial x}\right]_e = 0 \tag{32}$$

Where α is a user-defined weight factor. This equation can be discretized to obtain the following formula:

$$\hat{f}_e = F_P + \frac{1}{2\bar{u}_e}\left(P_P - P_E\right) \tag{33}$$

In this method, like all other methods discussed so far, Eq. (25) is used as the closure for p_e. Numerical results have shown that this set of closure equations removes the possibility of a checkerboard solution and provides strong coupling between pressure and velocity fields. Another analysis has shown that the use of momentum-variable formulation, instead of primitive variable formulation, improves the stability and accuracy of the solution especially in the solution of compressible flows with shock waves (Darbandi, 2004).

3.6 Method of proper closure equations (MPCE)

3.6.1 One-dimensional incompressible flow

Ashrafizadeh et al. (Ashrafizadeh et al., 2009) have shown that it is possible to develop a co-located numerical scheme without resorting to the convecting and convected velocity concepts, originally proposed by Rhie and Chow. The proposed method, called the method of proper closure equations (MPCE), employs a proper set of physically relevant equations to constrain the velocity and pressure at integration points. It has already been successfully implemented and used in the solution of steady 1-D inviscid incompressible and compressible flow problems (Ashrafizadeh et al., 2008, 2009) and steady 2-D viscous incompressible flow problems on both structured and unstructured grids (Alinia, 2011; Bakhtiari, 2008).

In this method, following the physical-based approach proposed by Schneider and Raw (Schneider et al., 1987) and modifications proposed by Karimian and Darbandi (Darbandi, 1997; Karimian, 1994a), a combination of non-conservative form of momentum and continuity equations is used to obtain an interpolation formula for the ip-velocity:

$$\left[momentum\ Eq.\right]_e - \alpha_u u_e \left[continuity\ Eq.\right]_e = 0 \tag{34}$$

which results in:

$$\left[\rho u \underbrace{\frac{\partial u}{\partial x}}_{UDS} + \rho u \underbrace{\frac{\partial u}{\partial x}}_{1} + \rho u^2 \frac{1}{A}\underbrace{\frac{da}{dx}}_{CDS} + \underbrace{\frac{\partial P}{\partial x}}_{CDS} - S^u\right]_e - \alpha_u u_e \left[\rho \underbrace{\frac{\partial u}{\partial x}}_{2} + \rho u \frac{1}{A}\underbrace{\frac{da}{dx}}_{CDS} - S^m\right]_e = 0 \tag{35}$$

Here S^u and S^m are artificial momentum and mass source terms, and a and α_u are the ip-cross sectional area and a scheme control parameter respectively. There are options available to the user at this stage. Using UDS or CDS Schemes for terms 1 and 2 and $\alpha_u = 0,\ 1,\ 2$, as discussed in (Rezvani, 2008), different formulas for u_e can be obtained. The most common formula is as follows:

$$u_e = U_P + \frac{P_P - P_E}{2\rho\bar{u}_e} + \frac{\Delta x}{2\rho\bar{u}_e}(S_e^u - \bar{u}_e S_e^m) \tag{36}$$

As mentioned earlier, the classical closure choice for the integration point pressure has been the linear approximation, i.e. Eq.(25). However, the MPCE employs relevant governing equations to obtain the required closures for all integration point quantities, including the pressure. The momentum equation is a natural choice for obtaining a proper closure equation for p_e. However, only the pressure gradient appears in the momentum equation and CDS-based discretization, physically proper for the pressure, results in wiggly solutions. As discussed in (Rezvani, 2010), by taking the divergence of the momentum equation, a pressure poisson equation for the pressure is obtained. The pressure Poisson equation is an appropriate constraint equation for the pressure discretization. Therefore, as compared to Eq. (34), the following closure equation is proposed for the integration point pressure:

$$\begin{bmatrix} Divergence\ of \\ Momentum\ Eq. \end{bmatrix}_e - \alpha_P \frac{4\overline{u}_e}{\Delta x}\left[Continuity\ Eq.\right]_e = 0 \tag{37}$$

Which results in:

$$P_e = \frac{P_P + P_E}{2} + \alpha_P \frac{\rho\overline{u}_e}{2}\left(U_P - U_E\right) + \alpha_P \frac{\rho\overline{u}_e^2}{2a_e}\left(A_P - A_E\right) + \frac{\Delta x^2}{4}\left[\left.\frac{\partial u}{\partial x}\right|_e + 2\alpha_P \frac{\overline{u}_e}{\Delta x}\right] S_e^m \tag{38}$$

Where $\alpha_P > 0$ is a scheme control parameter. Numerical test results have shown that the method works well with any nonzero positive value for α_P (Rezvani-2010).

3.6.2 One-dimensional compressible flow

Extension of the MPCE to compressible flow problems requires two additional tasks. First, the energy equation should also be solved in order to find the temperature filed. Second, depending on the chosen unknown variables, proper linearization is crucially important. Following approaches presented in (Darbandi et al., 2007; Karimian, 1994a), the Newton-Raphson linearization strategy is employed to linearize the nonlinear terms in the balance equations. For example, term pu in the energy equation is linearized as follows:

$$pu = \left(\rho Rt\right)u = \left(\rho u\right)Rt = R\left(ft\right) = R\left(\overline{f}\overline{t} + \overline{t}\overline{f} - \overline{ft}\right) \tag{39}$$

Closure equation for f_e can be easily obtained using the unsteady-compressible form of Eq. (34). First order upwind difference scheme is used for the discretization of momentum variable gradient terms. Use of $\alpha_u = 1$ in the general form of the closure for the momentum variable at the east face of the cell, results in the following formula for f_e:

$$f_e = \frac{2C\dfrac{\overline{\rho}_e}{\overline{\rho}_P}}{1+2C}F_P + \frac{C\left(P_P - P_E\right)}{\overline{u}_e\left(1+2C\right)} + \frac{f_e^\circ}{1+2C} + \frac{C\Delta x}{1+2C}\left.\frac{\partial\overline{\rho}}{\partial\tau}\right|_e + \frac{C\Delta x}{\overline{u}_e\left(1+2C\right)}\left(S_e^u - \overline{u}_e S_e^m\right) \tag{40}$$

Where, C is the Courant number defined as $C = \overline{u}\,\Delta\tau/\Delta x$ and superscript $^\circ$ stands for the values from previous time step.

Similarly, Closure equation for p_e can be obtained using the unsteady-compressible form of Eq. (37) as follow:

$$p_e = \frac{P_P + P_E}{2} + \frac{\alpha_p}{2}\overline{u}_e\left(F_P - F_E\right) + \frac{\alpha_p}{2}\frac{\overline{f}_e\overline{u}_e}{a_e}\left(A_P - A_E\right) + \frac{\Delta x^2}{4}\left[\left.\frac{\partial u}{\partial x}\right|_e + 2\alpha_p\frac{\overline{u}_e}{\Delta x}\right]S_e^m - \frac{\alpha_p}{2}\overline{u}_e\Delta x\left.\frac{\partial\overline{\rho}}{\partial\tau}\right|_e \tag{41}$$

The non-conservative form of the continuity equation in Eq. (6), in the absence of its source term, is proposed as a proper closure equation for the density (Darbandi et al., 1997; Karimian, 1994a). Here, in order to control the stability and accuracy of the code in both subsonic and supersonic regimes, a smart blending factor (β) is used which makes the equation hyperbolic in supersonic flow regions [Karimian, 1994a]:

$$\rho_e = \rho_P - \beta_e\frac{\Delta x}{2\overline{u}_e}\left[\frac{\partial\overline{F}}{\partial x} + \frac{\overline{f}}{a}\frac{\partial A}{\partial x} + \frac{\partial\overline{\rho}}{\partial\tau}\right]_e + \left(1-\beta_e\right)\left.\frac{\partial\overline{\rho}}{\partial x}\right|_e\frac{\Delta x}{2} \tag{42}$$

$$\beta_e = \frac{M_e^m}{M_e^m + 1} \tag{43}$$

where M_e is local Mach number at the "east" integration point and m=2 is suggested for the superscript m.

The final required closure equation is an interpolation formula for the integration point temperature. Here, the non-conservative form of the energy equation in the absence of the source term is a natural candidate (Darbandi et al., 1997) and one obtains the following expression:

$$t_e = \frac{2C}{1+2C}T_P + \frac{C\,\overline{p}_e}{\overline{f}_e c_v\left(1+2C\right)}\left(\frac{F_P}{\overline{\rho}_P} - \frac{F_E}{\overline{\rho}_E}\right) + \frac{C}{1+2C}\frac{\overline{p}_e\left(A_P - A_E\right)}{\overline{\rho}_e c_v a_e} + \frac{t_e^\circ}{1+2C} \tag{44}$$

The final discrete computational molecules for solving velocity, pressure and temperature fields are obtained after closure equations are substituted in Eq. (9):

$$a_P^{pp}P_P + \sum a_{nb}^{pp}P_{nb} + a_P^{pf}F_P + \sum a_{nb}^{pf}F_{nb} + a_P^{pt}T_P + \sum a_{nb}^{pt}T_{nb} = b_P^p \tag{45}$$

$$a_P^{ff}F_P + \sum a_{nb}^{ff}F_{nb} + a_P^{fp}P_P + \sum a_{nb}^{fp}P_{nb} + a_P^{ft}T_P + \sum a_{nb}^{ft}T_{nb} = b_P^f \tag{46}$$

$$a_P^{tt}T_P + \sum a_{nb}^{tt}T_{nb} + a_P^{tf}F_P + \sum a_{nb}^{tf}F_{nb} + a_P^{tp}P_P + \sum a_{nb}^{tp}P_{nb} = b_P^t \tag{47}$$

In this linear algebraic set, $a_P^{ff}, a_P^{fp}, \ldots$ are the influence coefficients and $b_P^p, b_P^f, \ldots$ are right hand side constant terms. Subscript nb stands for the immediate neighbors of node P (i.e. W and E). The first superscript refers to the relevant equation and the second superscript points to the relevant physical variable. The assembled linear equations can be solved using any direct or iterative solver. Here, the Gauss elimination method is used to solve the set of simultaneous equations. The coupled set of the algebraic equations might also be solved using a semi-implicit (segregated) solution strategy.

3.6.3 Two-dimensional incompressible flow

The MPCE has also been used to solve 2D, incompressible laminar flows on both structured and unstructured grids (Bakhtiari, 2008; Alinia, 2011). The implementation follows the basic philosophy already described in a 1D context. However, more complex interpolation formulas are required to take into account the effect of cell shape and orientation on balance equations. Implementation details are not discussed here for the sake of brevity.

4. One-dimensional test cases

4.1 Incompressible flow

Performance of the MPCE for solving incompressible and compressible flows is examined here through two different test cases. Steady incompressible flow in a constant area duct is the first test case which is used to examine the pressure-velocity coupling in MPCE. Quasi 1D flow in a convergent-divergent nozzle is another test case used to check the accuracy of the proposed method in inviscid incompressible flow problems.

4.1.1 Steady incompressible flow in a constant area duct

The 1D incompressible flow in a constant area duct is used to see if oscillatory solutions appear when the MPCE equations govern the discrete flow field. For this purpose, artificial element and volume sources/sinks are used in continuity and momentum equations. In a domain with 30 nodes, the artificial element source terms are located at the 10th and 20th cell-faces and control volume source terms are activated at the 10th and 20th nodal positions.

Numerical results show that the effects of sharp variations in velocity and pressure due to the artificial source terms are quickly damped out and MPCE works well even with $\alpha_p = 0$. Figures 5 and 6 show the effects of control-volume artificial sources on the numerical solution. These results show that numerical oscillations are developed in both velocity and pressure fields for $\alpha_p = 0$. However, oscillations are strongly damped for any non-zero value of α_p. Note that the notation "N-D" in these figures stands for "Non-Dimensional" and velocity is normalized with the inlet velocity and pressure is normalized using the exit pressure.

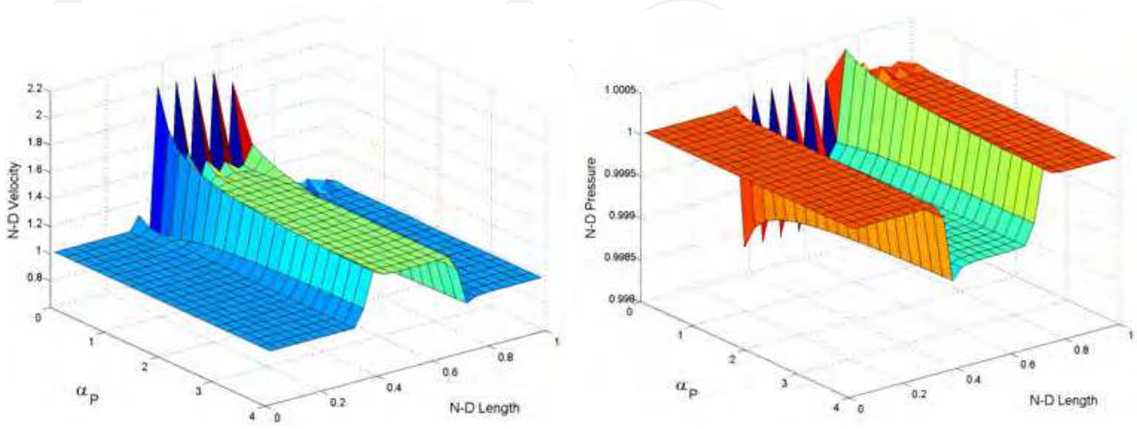

Fig. 5. Velocity and pressure fields in a constant area duct with control-volume mass source/sink.

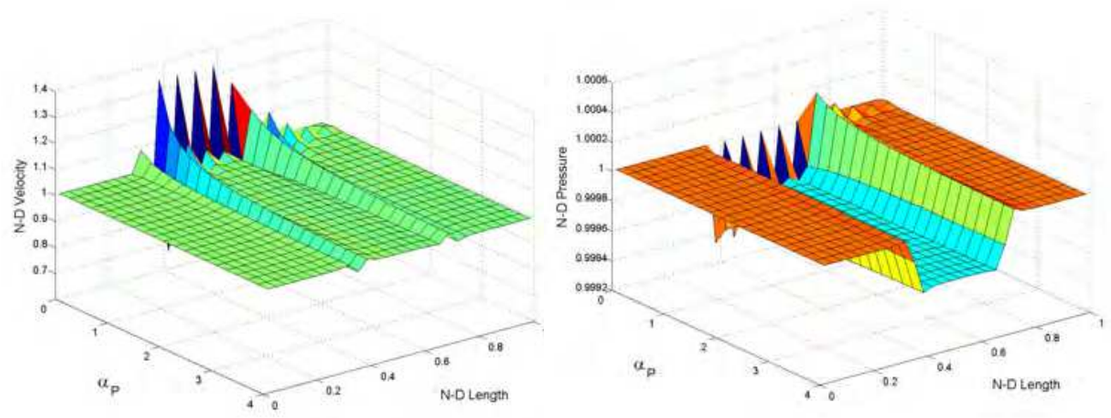

Fig. 6. Velocity and pressure fields in a constant area duct with control-volume momentum source/sink.

4.1.2 The quasi-1-D test case

Ideal flow in a converging-diverging nozzle is another test case to examine the performance of MPCE. Figure 7 compares the non-dimensional velocity and pressure distributions along the nozzle with the analytical solutions. Excellent agreement is observed.

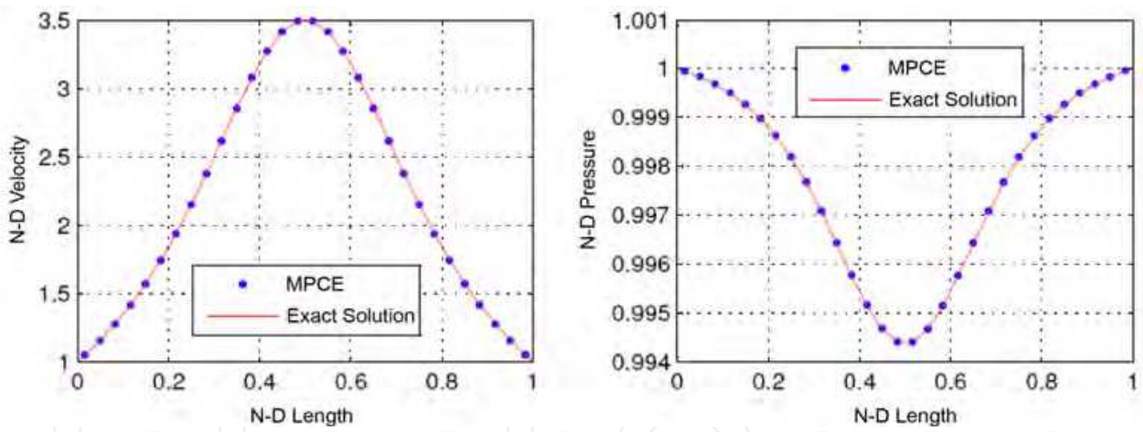

Fig. 7. Velocity and pressure field in a 1D converging-diverging nozzle ($\alpha_p = 1$).

4.2 Compressible flow

For compressible flow, performance of MPCE is examined in three different test problems. Steady subsonic compressible flow in convergent-divergent nozzle, steady compressible flow with normal shock in convergent-divergent nozzle and unsteady compressible flow with normal shock and expansion waves in a shock tube.

4.2.1 Steady subsonic compressible flow in a convergent-divergent nozzle

Results of solving subsonic compressible flow in a symmetric convergent-divergent nozzle with aspect ratio 2 using 51 nodes is shown in this section. For the boundary condition implementation, mass flow rate and the static temperature are specified at the inlet and the

static pressure is provided at the outlet. In order to assess the accuracy of the proposed method, numerical solutions corresponding to inlet Mach numbers of 0.05, 0.1, 0.15, 0.2, and 0.25 are presented in Fig. 8. Flow with the inlet Mach number of 0.3059, for which the nozzle is choked, is also considered. In this test case, $\alpha_p = 1$ is used and pressure, temperature, and density are nondimensionalized with the outlet pressure, inlet temperature, and inlet density, respectively.

4.2.2 Steady flow with shock waves

In the divergent section of the previous test case, normal shock waves appear for certain inlet boundary conditions while the position and the strength of the shock can be controlled by regulating the back pressure. Figure 9 presents the Mach number, non-dimensional pressure, temperature and density distributions along the nozzle for the pressure ratios (P_{outlet}/P_{inlet}) of 0.65, 0.75 and 0.85 using 81 nodes. It is seen that the normal shock is well captured using a few nodes in all cases and no numerical oscillation is developed along the nozzle. Note that this results are computed using $m = 2$ in Eq.(43) and α_p takes values lower than 1 in the supersonic parts of the solution domain and values higher than 1 in the subsonic regions.

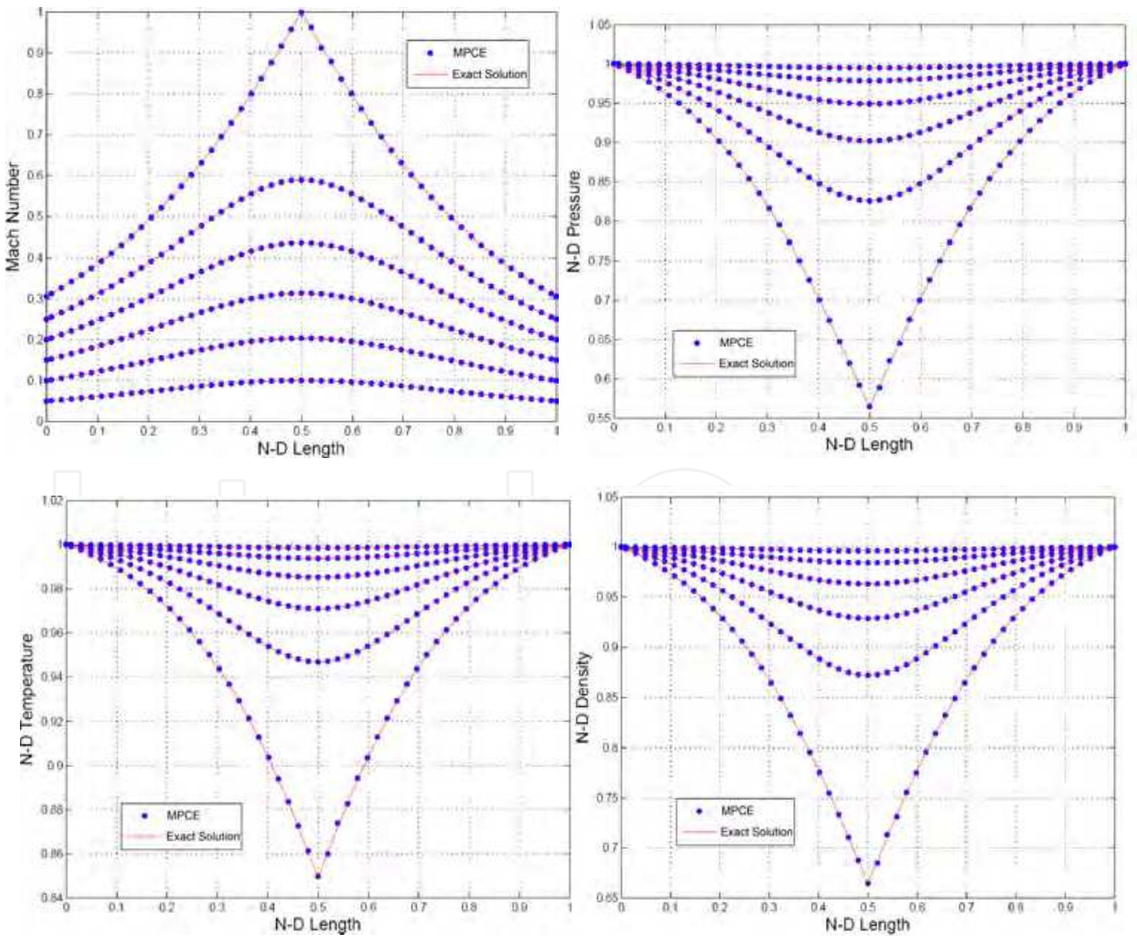

Fig. 8. Steady subsonic compressible flow in a convergent-divergent nozzle.

4.2.3 Unsteady compressible flow in a shock tube

As the final unsteady 1D test case with both compression and expansion waves, shock tube problem is discussed. The geometry shown in Fig.10 is a constant area duct divided into two regions separated by a diaphragm at the middle of the duct. At $\tau = 0$ the gas temperature is 298 K, the pressure at the right side of the membrane is 100 KPa and the pressure at the left side of the membrane is 1000 KPa. The time step for the marching numerical solution is equal to $\Delta\tau = 4 \times 10^{-6}$ seconds. Figure 11 shows the numerically calculated distributions of Mach number, non-dimensional pressure, temperature, and density after 0.42×10^{-3} seconds. Here, the Courant number is 0.229 which is computed using the maximum magnitude of velocity in the domain. The pressure, temperature and density are non-dimensionalized using the low pressure side values. Good agreement with the exact solution is observed.

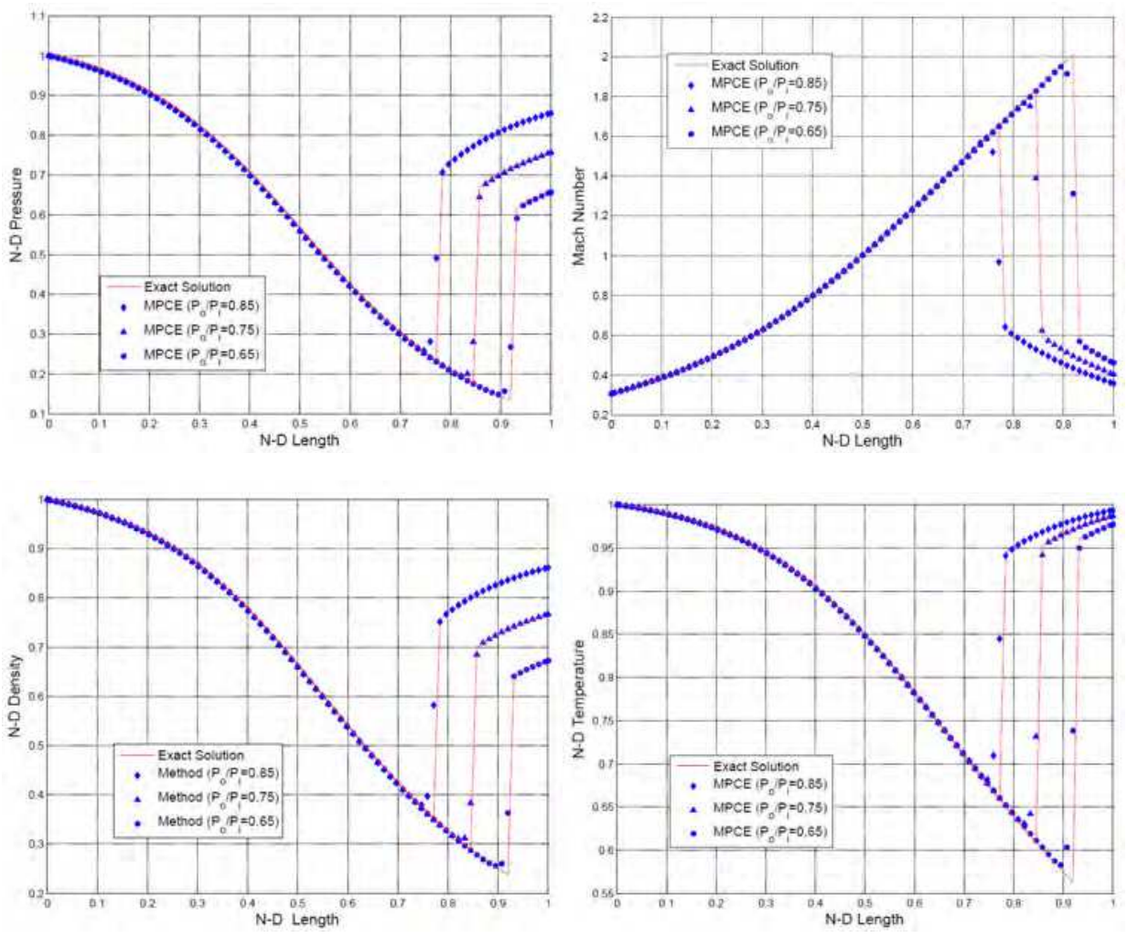

Fig. 9. Steady flow with shock waves in a convergent-divergent nozzle.

5. Two-dimensional incompressible flow test cases

The MPCE has also been used to solve many 2D benchmark test problems. Here, only the results for two standard test cases are presented.

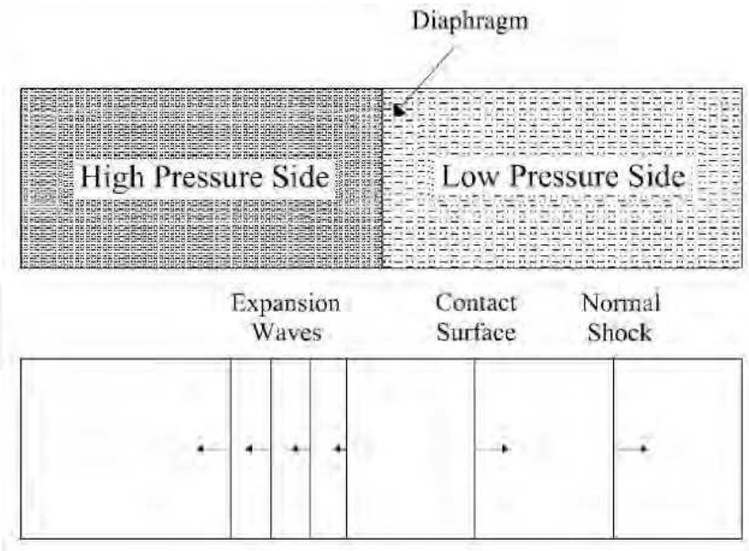

Fig. 10. Geometry and the flow pattern for the shock tube problem.

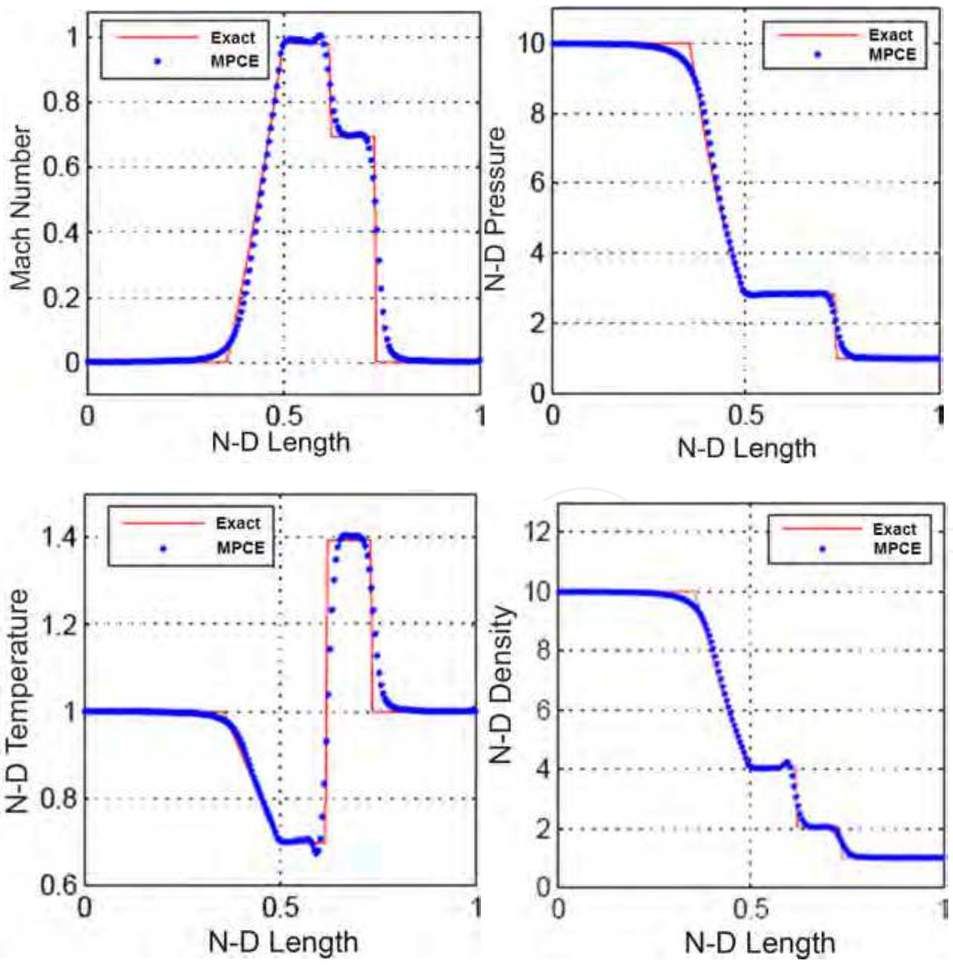

Fig. 11. Results of unsteady compressible flow in shock tube

5.1 Flow in a 2D lid-driven cavity

Flow in a lid-driven cavity, shown in Fig. 12, is a widely used test case for 2D steady incompressible flows governed by Navier-Stokes equations. Numerical solution via MPCE on an unstructured grid with 12656 triangular elements, shown in Fig. 13, is compared to the numerical results of Erturk (Erturk, 2005). Flow patterns at different Reynolds numbers are shown in Fig. 14. Excellent agreement between the calculated velocities at cavity centerlines and the benchmark results in Fig. 14 is also observed.

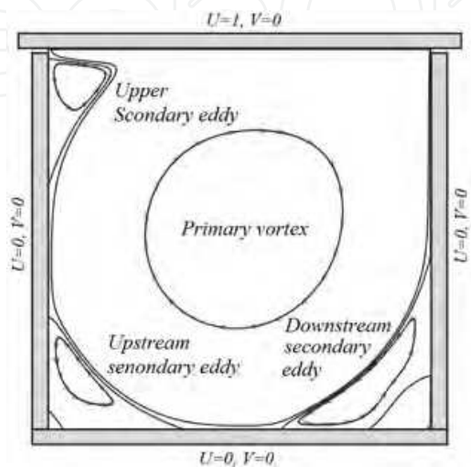

Fig. 12. Lid-driven cavity boundary conditions with an schematic of flow features.

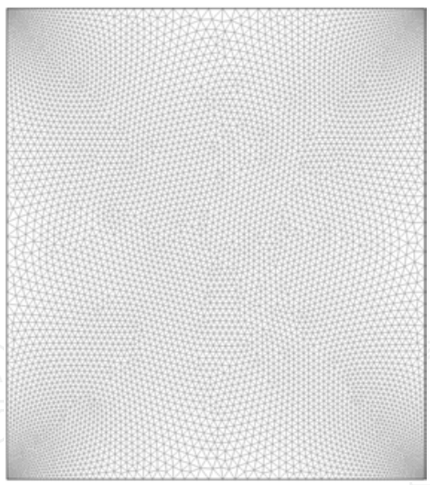

Fig. 13. Generated unstructured mesh for lid-driven cavity test case.

5.2 Flow over a backward facing-step

The backward step flow is another commonly used test case for numerical solution algorithms. The geometry of this test case is shown in Fig. 15. Forty nodes are used across the channel, 300 nodes are used from the step to 30h and 50 nodes are used from 30h to 50h along the channel. Nodes are distributed uniformly. Figure 16 shows the calculated streamlines at Re=800, in which a recirculation zone appears at the upper wall. Normalized locations of the re-attachment point at the lower wall (X1), the separation point at the upper

wall (X2), and the re-attachment point at the upper wall (X3) are compared with the results obtained by Gartling (Gartling, 1990) for flow at Re = 800. Comparison results are shown in Table 1 and excellent agreement is obvious (Erturk, 2008). A comparison has also been made between numerical results via MPCE and the benchmark results in (Gartling, 1990) and shown in Fig. 18. Again, excellent agreement is observed. Similar calculations and comparisons have also been made for a backward-step flow model with an inlet channel. Excellent results, not shown here, are also obtained in this test case.

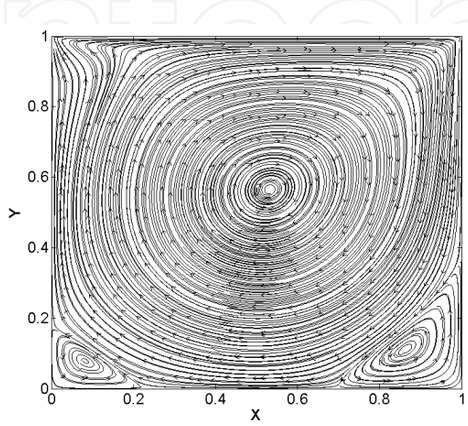

(a) Streamlines at Re = 1000.

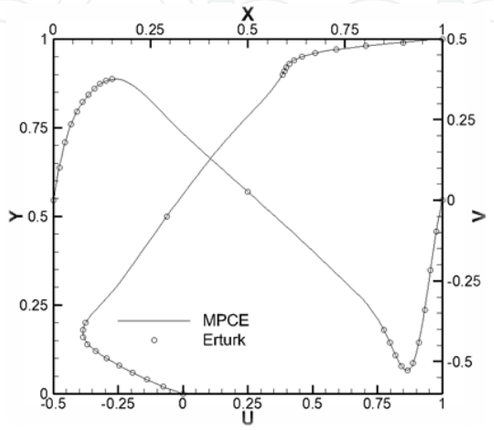

(b) Velocity Profiles at Re = 1000.

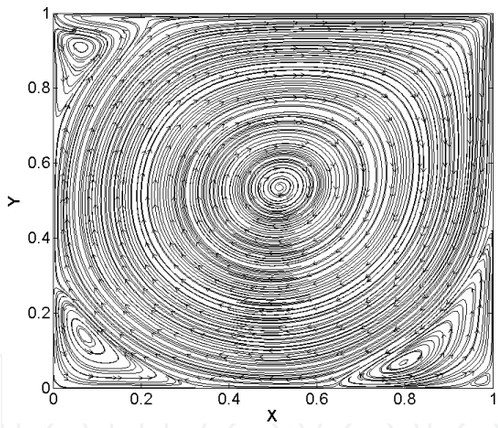

(c) Streamlines at Re = 5000.

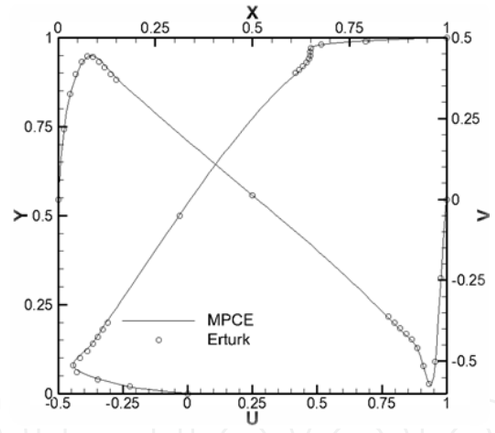

(d) Velocity Profiles at Re = 5000.

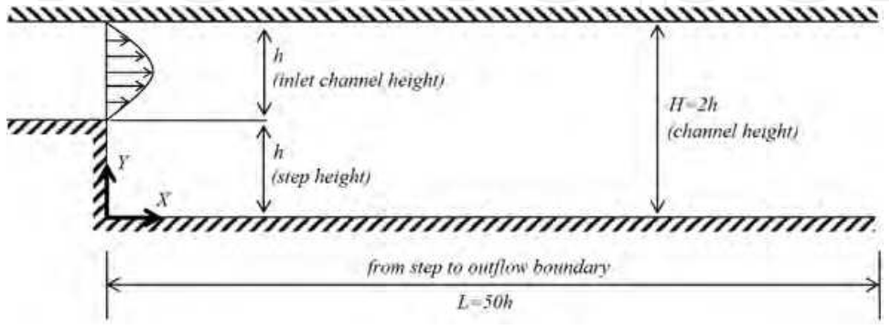

Fig. 14. Schematic view of the backward facing-step flow problem.

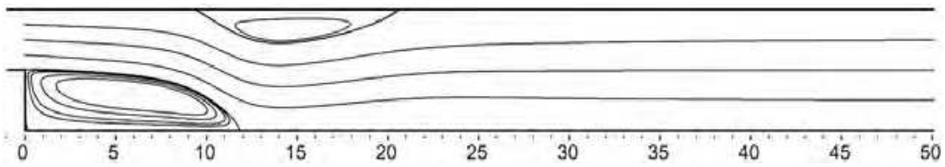

Fig. 15. Calculated streamlines in the backward-step flow problem at Re = 800.

	X1	X2	X3	X3 – X2
MPCE	12.0419	9.5528	20.8093	11.2565
Erturk	12.20	9.70	20.96	11.26

Table 1. Comparison of normalized X1, X2 and X3 locations and length of the first recirculating region on the upper wall (X3 – X2) for Re = 800

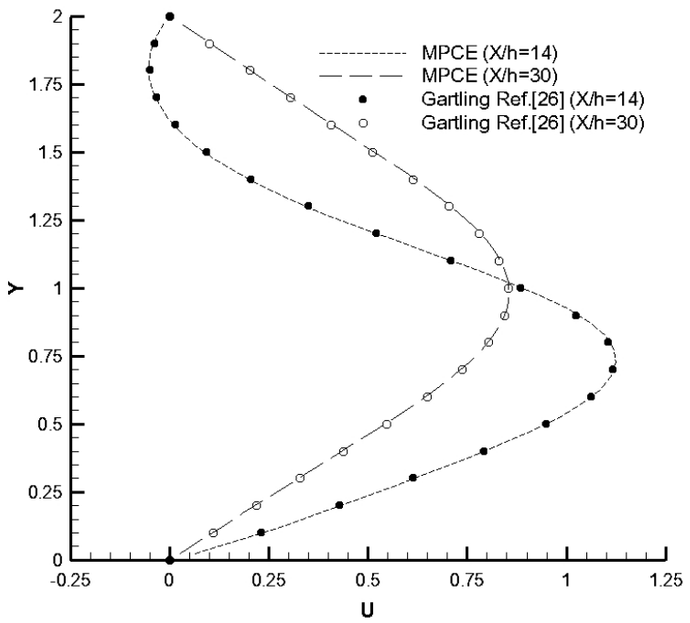

Fig. 16. Horizontal velocity profiles across the channel at X/h = 14 and 30 for Re = 800.

6. Conclusion

Different pressure-based finite volume discretization schemes for the solution of fluid flow problems are explained and compared in the context of co-located grid arrangements and a new scheme, called the Method of Proper Closure Equations (MPCE), is proposed. The proposed method is the only discretization scheme on co-located grids which employs only one definition for the integration point velocity and successfully solves incompressible as well as compressible flow problems. Simple one-dimensional test cases are presented to discuss different available schemes and the building blocks of MPCE. Implementation of the MPCE on 2D structured and unstructured grids has also been carried out but the details are not reported here for the sake of brevity. Numerical solutions via MPCE, however, are presented for both 1D and 2D problems which clearly show the satisfactory performance of the MPCE in the numerical solution of fluid flow problems.

7. References

Acharya, S; Baliga, B. R; Karki, K.; Murthy, J. Y.; Prakash, C. & Vanka, S. P. (2007). Pressure-Based Finite-Volume Methods in Computational Fluid Dynamics. *Journal of Heat Transfer*, Vol. 129, pp. 407-424

Alinia, B. (2011). Implementation of the Method of Proper Closure Equations on Two-Dimensional Unstructured Grids for Steady, Incompressible Viscous Problems, *M.Sc. Thesis*, Department of Mechanical Engineering, K.N.Toosi University of Technology, Tehran, Iran, (In Persian)

Alisadeghi, H. & Karimian, S. M. H. (2011a). Different Modelings of Cell-Face Velocities and Their Effects on the Pressure-Velocity Coupling, Accuracy and Convergence of Solution, *International Journal for Numerical Methods in Fluids*, Vol. 65, pp.969-988

Alisadeghi, H. & Karimian, S. M. H. (2011b). Comparison of Different Solution Algorithms for Collocated Method of MCIM to Calculate Steady and Unsteady Incompressible Flows on Unstructured Grids, *Computers and Fluids*, Vol. 46, 94-100

Ashrafizadeh, A.; Okhovat, S.; Pourbagian, M. & Raithby, G. D. (2011). A Semi-Coupled Solution Algorithm in Aerodynamic Inverse Shape Design, *Inverse Problems in Science and Engineering*, Vol. 19, No. 4, pp. 509-528, ISSN 1741-5985

Ashrafizadeh, A.; Rezvani M.; & Bakhtiari, B. (2008). A New Co-located Pressure-Based Finite Volume Method, *16th Annual Conference of the CFD Society of Canada*, Saskatoon, Saskatchewan, Canada

Ashrafizadeh, A.; Rezvani M.; & Bakhtiari, B. (2009). Pressure-Velocity Coupling On Co-Located Grids Using the Method of Proper Closure Equations, *Numerical Heat Transfer; Part B*, Vol. 56, pp.259–273

Bakhtiari, B. (2008). Decoupling of Pressure and Velocity in the Numerical Simulation of Incompressible Flows: A review. *M.Sc. Thesis*, K.N.Toosi University of Technology, Tehran, Iran, (In Persian)

Chterental, I. (1999). Two-Dimensional Euler Equations Solver, *M.Sc. Thesis*, Graduate Department of Aerospace Science and Engineering, University of Toronto, Toronto, Canada

Darbandi, M. & Schneider, G. E. (1997). Momentum Variable Procedure for Solving Compressible and Incompressible Flows. *AIAA Journal*, Vol. 35, pp. 1801-1805

Darbandi, M. & Mokarizadeh, V. (2004). A Modified Pressure-Based Algorithm to Solve Flow Fields With Shock and Expansion Waves, *Numerical Heat Transfer, Part B*, Vol. 46, pp.497–504

Darbandi, M.; Roohi, E. & Mokarizadeh, V. (2007). Conceptual Linearization of Euler Governing Equations to Solve High Speed Compressible Flow Using a Pressure-Based Method, *Numerical Methods for Partial Differential Equations*, DOI 10.1002, pp 583-604

Erturk, E.; Corke, T. C. & Gökçöl, C. (2005). Numerical Solutions of 2-D Steady Incompressible Driven Cavity Flow at High Reynolds Numbers, *Int. J. Numer. Meth.* Fluids, Vol. 48, pp. 747-774

Erturk, E. (2008). Numerical Solutions of 2-D Steady Incompressible Flow Over a Backward Facing Step, Part I: High Reynolds Number Solutions, *Int. J. Computers & Fluids*, Vol. 37, pp. 633-655

Gartling, D. K. (1990). A Test Problem for Outflow Boundary Conditions – Flow Over a Backward Facing Step, *Int. J. Numer. Meth. Fluids*, Vol. 11, pp. 953-969

Karimian, S. M. H. & Schneider, G. E. (1994a). Application of a Control-Volume-Based Finite-Element Formulation to the Shock Tube Problem, *AIAA Journal*, Vol.33 No.1, pp. 165-167

Karimian, S. M. H. & Schneider, G. E. (1994b). Pressure-based Computational Method for Compressible and Incompressible Flows, *Journal of Thermophysics and Heat Transfer*, Vol.8, No.2 , pp. 267-274

Patankar, S. V. (1980). *Numerical Heat Transfer and Fluid Flow*, Hemisphere Publishing Corporation, Washington, D. C.

Rezvani, M. (2008). A New Pressure-Based Computational Method for Solving Fluid flow at all speeds, M.Sc. Thesis, Department of Mechanical Engineering, K.N.Toosi University of Technology, Tehran, Iran, (In Persian)

Rezvani, M. & Ashrafizadeh, A. (2010). Numerical Simulation of the Inter-Equation Couplings in All-Speed Flows via the Method of Proper Closure Equations, *Numerical Heat Transfer; Part A*, Vol. 58, pp. 1–20

Rhie, C.M. & Chow, W. L. (1983). A Numerical Study of the Turbulent Flow Past an Isolated airfoil With Trailing Edge Separation. *AIAA Journal*, Vol. 21, pp. 1525-1532

Schneider, G. E. & Raw, M. J. (1987a). Control Volume Finite-Element Method For heat Transfer and Fluid Flow Using Colocated Variables-1. Computational Procedure. *Numerical Heat Transfer, part B*, Vol. 11, pp. 363-390

Schneider, G. E. & Raw, M. J. (1987b). Control Volume Finite-Element Method For heat Transfer and Fluid Flow Using Colocated Variables-2. Application and Validation. *Numerical Heat Transfer, part B*, Vol. 11, pp. 391-400

IntechOpen

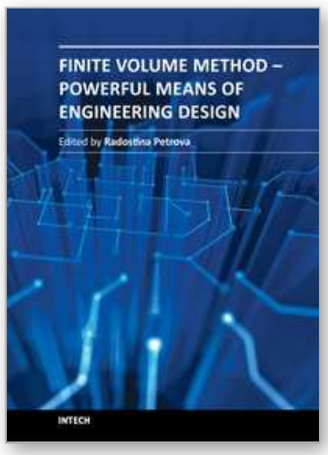

Finite Volume Method - Powerful Means of Engineering Design
Edited by PhD. Radostina Petrova

ISBN 978-953-51-0445-2
Hard cover, 370 pages
Publisher InTech
Published online 28, March, 2012
Published in print edition March, 2012

We hope that among these chapters you will find a topic which will raise your interest and engage you to further investigate a problem and build on the presented work. This book could serve either as a textbook or as a practical guide. It includes a wide variety of concepts in FVM, result of the efforts of scientists from all over the world. However, just to help you, all book chapters are systemized in three general groups: New techniques and algorithms in FVM; Solution of particular problems through FVM and Application of FVM in medicine and engineering. This book is for everyone who wants to grow, to improve and to investigate.

How to reference
In order to correctly reference this scholarly work, feel free to copy and paste the following:

A. Ashrafizadeh, M. Rezvani and B. Alinia (2012). Use of Proper Closure Equations in Finite Volume Discretization Schemes, Finite Volume Method - Powerful Means of Engineering Design, PhD. Radostina Petrova (Ed.), ISBN: 978-953-51-0445-2, InTech, Available from: http://www.intechopen.com/books/finite-volume-method-powerful-means-of-engineering-design/use-of-proper-closure-equations-in-finite-volume-discretization-schemes

INTECH
open science | open minds

InTech Europe
University Campus STeP Ri
Slavka Krautzeka 83/A
51000 Rijeka, Croatia
Phone: +385 (51) 770 447
Fax: +385 (51) 686 166
www.intechopen.com

InTech China
Unit 405, Office Block, Hotel Equatorial Shanghai
No.65, Yan An Road (West), Shanghai, 200040, China
中国上海市延安西路65号上海国际贵都大饭店办公楼405单元
Phone: +86-21-62489820
Fax: +86-21-62489821

© 2012 The Author(s). Licensee IntechOpen. This is an open access article distributed under the terms of the Creative Commons Attribution 3.0 License, which permits unrestricted use, distribution, and reproduction in any medium, provided the original work is properly cited.

IntechOpen

IntechOpen